Controllable coupling between ultra-high-Q microtoroid and graphene for filtering and switching applications

By *Huibo Fan, Xun Zhang, Hao Li, Jinyi Zhao, Yanhua Zhai, Yong Hu, Shiyue Hua, Jianming Wen, Xiaoshun Jiang,* and Min Xiao*

[*] Dr. H. Fan, X. Zhang, Hao Li, Jinyi Zhao, Prof. X. Jiang. Dr. Y. Hu. Dr. S. Hua, Prof. M. Xiao
National Laboratory of Solid State Microstructures, College of Engineering and Applied Sciences, School of Physics, Nanjing University, Nanjing 210093, China
E-mail: jxs@nju.edu.cn

[*] Dr. H. Fan
College of Physics Science and Technology, Yangzhou University, Yangzhou 225002, China

[*] Prof. Yanhua Zhai, Prof. Jianming Wen
Department of Physics, Kennesaw State University, Marietta, Georgia 30060, USA

[*] Prof. M. Xiao
Department of Physics, University of Arkansas, Fayetteville, Arkansas 72701, USA

Keywords: controllable coupling, microcavity, graphene, filter, switch

Abstract: Whispering-gallery-mode microresonators have found impactful applications in various areas due to their remarkable properties such as ultrahigh quality factor (Q factor), microscale mode volume, and strong evanescent field. In particular, they have enjoyed an increasing attention in the field of on-chip optical filters and modulators, given controllable tuning of the Q factor by interfacing with low-dimensional materials. Among many WGM resonators of different shapes and materials, on-chip silica microtoroids on silicon pillars are expected to exhibit better performance, yet this is to be demonstrated in bandwidth tunability and resonant wavelength shift. Here, we report such an experimental demonstration with a hybrid structure formed by an ultrahigh-Q microtoroid and a graphene monolayer. Thanks to the strong interaction of the evanescent wave with the graphene, the structure allows the Q factor to be controllably varied in the range of $3.9 \times 10^5 \sim 6.2 \times 10^7$ by engineering optical absorption via changing the gap distance in between. At the same time, a shift in resonant wavelength approximately 32 picometer was also observed. Besides, the scheme enables us to approach the critical coupling with a coupling depth of 99.6% at the critical coupling point. As potential applications in integrated opto-electronic devices, we further use the system to realize a tunable filter with tunable bandwidth from 116.5 MHz to 2.2 GHz as well as an optical switch with a maximal extinction ratio of 31 dB.

1. Introduction

By confining light in a tiny volume with high quality (Q) factors so as to enhance the interaction of light with matters within or surrounding the cavity, whispering-gallery-mode (WGM) microcavities have shown promising applications as a crucial element for a variety of devices ranging from micro-lasers, micro-sensors, micro-filters, to micro-modulators. Owing to the full compatibility with the mature CMOS procedure, they are becoming the basic building blocks of integrated photonic systems. As such, over decade tremendous progress has been made in the development of miniature photonic information processing technologies based on microscale high-Q microcavities. Nevertheless, many of these applications rely on the capability of tuning the Q-factors as well as shifting the resonant wavelengths. For instance, high-Q microcavities are highly sensitive to various environmental factors such as

temperature, humidity, and any particles or absorbers. To enforce the sensing applications, new methods including photothermal mapping and phase shift microcavity ring down spectroscopy have recently been exploited to change Q-factor and resonant wavelength. Alternatively, the ability of controlling tuning these two factors becomes critical for a wide range of applications, e.g., in the design of ultra-short pulsed lasers and optical modulators. Although some progress has been made in utilizing a saturable absorber to reach the goals, yet, it is still quite challenging to realize these opto-electronic devices with desired tunability, partly due to the technical difficulty in integrating high-Q microcavities with such absorption media in a controllable way.

On the other hand, given excellent optical properties including linear optical absorption, graphene monolayers as ideal two-dimensional quantum materials have aroused great interest in many photonic applications, such as polarization controllers, photodetectors, modulators, and pulsed lasers, for better performance. However, due to technical complexity, these devices are usually unreachable or unoptimizable in conventional material systems. Moreover, for various applications, it is required to have the ability to transfer and integrate graphene onto fiber end faces or wafer surfaces. Alternatively, there is a high demand for methods of integrating graphene with chip-based photonic devices, e.g., waveguides and optical microcavities. Along this direction, recent efforts are made towards optoelectronic devices based upon a graphene-clad photonic crystal nanocavity to achieve resonant optical bistability, regenerative oscillation, and four-wave mixing. Besides, a graphene electro-optic modulator rooted in a silicon nitride microring resonator was also demonstrated where the modulation bandwidth of 30 GHz was reported. Despite these impressive results, it is still lack of a systematic study of the light-matter interaction between a WGM microcavity and graphene, especially the realization of a tunable interaction strength.

By using graphene as a tunable absorber, here we realize controllable coupling strength for a hybrid structure composed of an ultra-high-Q microtoroid cavity and a graphene monolayer through changing the Q factor in orders of magnitude. With this hybrid structure, we can accurately control the gap between the microtoroid and graphene through high-precision displacements. Thanks to the optical absorption of graphene induced by the strong evanescent wave outside of the microtoroid, the Q factor can be altered from 6.2×10^7 to 3.9×10^5 as gradually reducing the microtoroid-graphene gap. Meanwhile, the microcavity resonant wavelength is shifted towards the longer wavelength, and exhibits a maximal shift of approximately 32 pm. As the graphene is gradually moved away from the microtoroid surface, the microcavity Q factor as well as its resonant wavelength are restored to their original values. In addition, we demonstrate the critical coupling using this hybrid structure, and obtain the coupling depth of 99.6% at the critical coupling point. Besides, we further realize a tunable filter with a variable bandwidth in the range of 116.5 MHz ~ 2.2 GHz, and an optical switch with a maximal extinction ratio of 31 dB. These demonstrations indicate that our hybrid structure provides a good reference for realization of integrated opto-electronic devices such as on-chip optical modulators and optical filters.

2. Results and Discussion

Since the field distribution of the microcavity resonance is essential for the applications, we first carried out theoretical analysis on the optical properties of this hybrid system, and in particular, we focused on the additional losses of different cavity resonant modes induced by the optical absorption of the graphene monolayer. We hence conducted a finite-element simulation in which the graphene monolayer was treated as a 0.35-nm-thick dielectric layer, and the corresponding optical properties were taken from the Reference [23]. For the microtoroid cavity, its principal (denoted by D in Figure 2a) and minor (d) diameters are,

respectively, measured to be 56 μm and 6 μm. The total cavity loss is mainly from two sources, that is, the intrinsic loss of the microtoroid and the extra loss caused by the graphene. Mathematically, the total loss is modeled by the relation $1/Q = 1/Q_0 + 1/Q_{gra}$, where Q_0 is the intrinsic Q factor while Q_{gra} is the effective Q factor describing the absorption of graphene. In the experiment, we noticed that in comparing with high-order modes, the fundamental mode of the microcavity was located near the middle of the ring, and yielded a weaker coupling with the graphene. For instance, the Q factors of the fundamental modes are, respectively, decreased to be approximately 3.0×10^6 and 2.0×10^7 for the transverse electric (TE) and transverse magnetic (TM) modes, when the gap distance between the microtoroid and graphene approaches zero. The TE mode profile is schematically illustrated in Fig. 1a. In contrast, the third-order modes were distributed near the edge of the ring and consequently, yielded stronger coupling with the graphene. Alternatively, a larger variation of the Q factor is expected in the measurement. Indeed, as the microtoroid-graphene gap is almost zero, the Q factors are reduced to the minimum values of approximately 8.8×10^4 and 6.0×10^5, respectively, for the TE and TM modes. In Fig. 1c we depicted such TE mode distribution. As a comparison, when the gap disappears, Fig. 1b shows the second-order TE mode profile subject to the interaction with the graphene, where Q drops to approximately 2.3×10^5 (1.7×10^6 for the TM mode). Note that this plot corresponds to the simulated data shown in Fig. 1d. From the physical point of view, one expects that the total Q is dominated by Q_0 when the graphene is far from the microtoroid, but dominated by Q_{gra} when the gap is small. According to our simulation given in Fig. 1d, this compound system would permit the maximal wavelength shift of approximately 41 pm.

To verify our numerical predictions, an ultra-high-Q microtoroid was fabricated through a series of steps of micro-nano fabrication techniques,[24] whose scanning electron micrograph was given in Fig. 2b. The monolayer graphene was mechanically transferred to a specially designed silica substrate,[22,25] as shown in Figs. 2c and 2d. The details of the fabrication processes were presented in the Experimental Section. To form the proposed hybrid scheme, as illustrated in Fig. 2a, the microtoroid cavity was inversely mounted for the convenience of observation and measurement. The gap between the microtoroid and the graphene was precisely controlled through nano-position precision stages. The coupling was then investigated by injecting a probe light which was developed from a narrow-linewidth tunable diode laser operating at approximately the telecom band 1550 nm. In order to characterize this microtoroid-graphene composite structure, in the experiment we first displaced the graphene far enough from the microtoroid to ensure no influence of the graphene absorption on the cavity modes. Under such an arrangement, we scanned the laser wavelength to identify an appropriate cavity mode which resonantly couples with the input laser to yield an ultra-high Q. In this work, the initial intrinsic Q of the fabricated microtoroid was measured to be 6.2×10^7 at the 1570.0-nm wavelength. We then slowly moved the graphene close to the microtoroid surface and recorded the corresponding transmission power spectra in the output port by using a digital oscilloscope. The reduced gap resulted in the increased interaction between the evanescent wave and electron transition in graphene, which in turn broadened the cavity resonance linewidth. Consequently, this led to a significant reduction of the Q value. The cavity loss reached the maximum when the graphene exactly touched the microtoroid (i.e., the gap went to zero), and yielded the smallest Q of 3.9×10^5. By reversing the procedure through moving the graphene away from the cavity, we observed that Q reinstated its original value of 6.2×10^7 in the end.

The evolution of the probe transmission spectra was displayed in Fig. 3a in terms of the gap separation distance, which clearly showed the linewidth broadening along with the wavelength shift of the cavity resonance. The corresponding variations of the measured Q

factors and the resonant wavelength shift were plotted in Figs 3b and 3c, respectively. It is worthwhile to emphasize again that in the whole observation, the microtoroid Q can be reversibly changed in the range of 6.2×10^7 to 3.9×10^5 without degradation. In addition, to make sure that the observed Q variation was unaffected by the silica substrate film under the graphene, we also fabricated a similar silica microdisk with no graphene coating and used it for the same experimental procedure described above. It turns out that no obvious spectral changes were recorded in the transmission spectrum, implying no additional loss induced by the silica film. From Fig. 3a, it becomes also clear that owing to the optical absorption of graphene, the resonant wavelength of the microtoroid was shifted to the longer wavelength band by gradually diminishing the gap, and vice versa. This property is highly beneficial for the realization of optical modulation as well as optical switching. The obtained maximal shift was approximately 32 pm with the tunable bandwidth of 3.9 GHz. For comparison, the shift of the resonant wavelength in the latter experiment with the graphene-free microdisk was less than 1 pm, which in turn highlights that the resonant wavelength change in the former experiment was indeed a result of the graphene absorption.

The fabricated microtoroid is suitable for two critical coupling conditions when the fiber taper is moved in the vertical direction around the microtoroid. This led us to use the second-order TE mode in the numerical simulations in order to to fit the variations of the measured Q and resonant wavelength. The simulation curve turns out to match the experimental data well, as shown in Fig. 3b. The slight difference between simulation and experiment becomes apparent when the gap is close to zero. The deviation stems from the fact that the graphene was not entirely or uniformly coated on the microdisk during the fabrication process, as evidenced in Fig. 2c. This alternatively resulted in a slight degradation for the graphene absorption in the hybrid structure. To confirm this, we further made additional measurements on the transmission spectra of different WGMs, whose results are similar to those described above.

In a resonator-fiber taper system, the critical coupling is a unique position in which the output transmission drops to zero on resonance.[26] This behavior can be used for efficient loading of the matched fiber taper modes into the resonator while filtering unwanted modes in the applications of tunable filters or couplers.[27,28] Interestingly, the microtoroid-graphene hybrid structure developed here is an ideal setup to look at the critical coupling condition. To approach this condition, experimentally, prior to the reduction of the microtoroid-graphene gap, the taper-microtoroid subsystem was first biased into the over-coupled regime with the transmission of 50%. Figure 4a shows the relationship between the resonant transmission and the gap change. The apparent minimal transmission occurs at the gap around 1 μm with a coupling depth of approximately 99.6%. As the cavity linewidth would be affected by the light-graphene interaction, it is instructive to understand the power transmission as a function of the linewidth of the cavity resonant mode. It is known that after critical coupling, the linewidth would be broadened along with moving the graphene closer to the microtoroid. This trend has been verified in our experiment and the comparison between theory and experiment is provided in Fig. 4b.[26] We notice that when the linewidth is larger than 0.6 GHz (corresponding to $Q = 3.2 \times 10^5$), there appears a discrepancy between the experiment and the simulation, which is due to the large uncertainties present in the transmission spectra as the gap approaches zero. As a potential application by exploiting the critical coupling effect, we continued to experiment a bandwidth-tunable filter with this system. The set of measurements are shown in Fig. 5. As one can see, when decreasing the gap, the full width at half maximum (FWHM) of the transmitted spectrum becomes enlarged. In the experiment, we have achieved the tunable filter with a bandwidth of 116.5 MHz up to 2.2 GHz.

Given the easy access to the resonant wavelength shift and critical coupling, another potential application is to implement optical switching. The experimental results are given in Fig. 6. Experimentally, we first displaced the graphene far away from the microtoroid. A signal light operated at the wavelength of 1575.2 nm was thermally locked to the WGM resonance to yield zero transmittance. We then quickly brought the graphene close enough to the microtoroid. A near unity transmission at the input signal wavelength was observed, owing to the off resonance between the microtoroid and fiber taper (induced by the resonant wavelength shift). Subsequently, we utilized a proper rectangular wave with a fixed 1-Hz repetition rate along with the square pulses with tunable width to accurately control the high-precision piezoelectric displacement for fine scanning of the gap in the range of 722 nm ~ 0 nm (indicated by the red curve in Fig. 6b). The repeated back-forth shifting of the resonant wavelength thus functions as optical switching. As shown in Fig. 6a, the maxima of the normalized transmission spectra drop from unit to almost 0 sharply when the pulse width of the rectangular wave changes from 0.5 s to 0.01 s. Such a dramatic change gives rise to a high extinction ratio with the maximum of 31 dB, as shown in Fig. 6c, in this work. Note that Fig. 6b also shows the possibility to obtain the amplified output spectrum when the pulse width of the rectangular wave was set to 0.5 s. Another thing that shall be pointed out is that The response time (什么响应时间啊?) was approximately 21 ms here, whcih is limited by the response speed of the employed high-precision piezoelectric displacement.

3. Conclusion

In summary, by designing a hybrid structure consisting of an on-chip ultra-high-Q silica microtoroid and graphene, we have carried out a systematic investigation on the variations of Q and cavity resonant wavelength induced by the controllable optical absorption of the graphene. In the experiment, the microtoroid Q could be reversibly changed between 6.2×10^7 and 3.9×10^5 through tuning the gap between the two subsystems. Due to the evanescent wave interacting with the graphene, the cavity resonant wavelength is also shifted up to approximately 32 pm. Thanks to this perfect system, the critical coupling condition can be well approached with a sufficiently high coupling depth of 99.6% at the critical coupling point. As potential applications, we further demonstrated a tunable optical filter with a variable bandwidth in the range of 116.5 MHz ~ 2.2 GHz as well as an optical switch with a maximal extinction ratio of 31 dB. These demonstrations alternatively show that this hybrid design could become a good platform for the realization of integrated opto-electronic devices such as on-chip optical filters and optical switching.

4. Experimental Section

Sample fabrication: The ultra-high-Q microtoroid resonator was fabricated through a series of steps which involve photolithography, hydrofluoric acid etching, xenon difluoride etching, and carbon dioxide laser reflow.[24] In our design, the ultra-high-Q microcavity was placed on the corner of a silicon wafer to ease the measurements. The graphene monolayer was provided by XFNANO Materials Tech Co., Ltd. (Nanjing, China) and it was grown via chemical vapor deposition. In the experiment, this graphene monolayer was mechanically transferred to a specially designed silica substrate, i.e., a microdisk with the principal diameter of ~ 60 μm and the thickness of 0.8μm,[22] as shown in Figs. 2c and 2d. Specifically, Fig. 2c pictures the top-view (plus zoomed red-frame inset), zoomed side-view (yellow-frame inset), and magnified scanning electron micrograph of the graphene coated on the microdisk. The corresponding Raman spectrum measured at the wavelength of 532 nm for the graphene is shown in Fig. 2f. Here, the G and 2D peaks both follow the Lorentzian lineshapes and are, respectively, located at 1593.5 cm^{-1} and 2684.6 cm^{-1}. Based on the relative intensities of the G and 2D peaks as well as their Lorentzian profiles, the presence of only a single-layer graphene is thus confirmed.[25] To provide a necessary protection during the transfer process, a poly

methyl methacrylate (PMMA) layer was first coated on the graphene. After the transfer the PMMA was then dissolved by acetone. The specially designed silica microdisk substrate with 0.8-μm thickness was used to exclude other factors with adverse effects, such as the absorptions due to the silica and silicon substrates. These procedures ensure that only controllable coupling between the microtoroid and graphene would be obtained in experiment.

Optical measurement: Figure 2a gives an intuitive diagram of the experimental setup. As we can see, the inversely mounted microtoroid cavity was fabricated on the corner of the silicon wafer and was positioned right above the graphene. This geometrical arrangement was designed for the convenience of observation and measurement. In our experiment, a key was to keep the microtoroid, graphene, and fiber taper parallel throughout the whole measurement. This was realized with use of high-precision piezoelectric displacements. As we mentioned in the main text, the probe light coupling into the microtoroid cavity was a narrow-linewidth tunable diode laser operated at approximately 1550 nm. To adjust the light beam, a polarization controller and a variable optical attenuator were employed in the optical path. The adjusted field was then launched into the optical fiber taper. The fiber taper here has twofold purposes. That is to evanescently couple the laser light into the microtoroid on one hand, and to couple the signal light emitted from the cavity out to an oscilloscope for monitoring, on the other. As illustrated in Fig. 2a, the gap appearing between the microtoroid and graphene was precisely controlled by nano-position translation stages. When moving the graphene towards the microtoroid surface, the reduction of the gap leads to the increased cavity loss. Figures 2d and 2e are the top- and side-view optical microscope images of the hybrid structure, respectively.

Acknowledgements
((Acknowledgements, general annotations, funding. Other references to the title/authors can also appear here, such as "Author 1 and Author 2 contributed equally to this work."))

Y.-H. Z. and J.W. were supported by the US NSF EFMA-1741693, US NSF 1806519, and Kennesaw State University.

Received: ((will be filled in by the editorial staff))
Revised: ((will be filled in by the editorial staff))
Published online: ((will be filled in by the editorial staff))

References

[1] K. J. Vahala, *Nature* **2003**, *424*, 839.
[2] T. J. Kippenberg, K. J. Vahala, *Opt. Express* **2007**, *15*, 17172.
[3] M. L. Gorodetsky, A. A. Savchenkov, V. S. Ilchenko, *Opt. Lett.* **1996**, *21*, 453.
[4] S. Yang, Y. Wang, H. Sun, *Adv. Opt. Mater.* **2015**, *3*, 1136.
[5] Q. Ma, T. Rossmann, Z. Guo, *Meas. Sci. and Technol.* **2010**, *21*, 025310.
[6] K. D. Heylman, R. H. Goldsmith, *Appl. Phys. Lett.* **2013**, *103*, 211116.
[7] M. I. Cheema, S. Mehrabani, A. A. Hayat, Y.-A. Peter, A. M. Armani, A. G. Kirk, *Opt. Express* **2012**, *20*, 9090.
[8] L. Shao, X.-F. Jiang, X.-C. Yu, B.-B. Li, W. R. Clements, F. Vollmer, W. Wang, Y.-F. Xiao, Q. Gong, *Adv. Mater.* **2013**, *25*, 5616.
[9] R. R. Nair, P. Blake, A. N. Grigorenko, K. S. Novoselov, T. J. Booth, T. Stauber, N. M. R. Peres, A. K. Geim, *Science* **2008**, *320*, 1308.
[10] J. M. Dawlaty, S. Shivaraman, J. Strait, P. George, M. Chandrashekhar, F. Rana, M. G. Spencer, D. Veksler, Y. Chen, *Appl. Phys. Lett.* **2008**, *93*, 131905.

[11] F. Bonaccorso, Z. Sun, T. Hasan, A. C. Ferrari, *Nature Photon.* **2010**, *4*, 611.
[12] Q. Bao, H. Zhang, B. Wang, Z. Ni, C. H. Y. X. Lim, Y. Wang, D. Y. Tang, K. P. Loh, *Nature Photon.* **2011**, *5*, 411.
[13] F. Xia, T. Mueller, Y.-M. Lin, A. Valdes-Garcia, P. Avouris, *Nature Nanotech.* **2009**, 4, 839.
[14] M. Liu, X. Yin, E. Ulin-Avila, B. Geng, T. Zentgraf, L. Ju, F. Wang, and X. Zhang, *Nature* **2011**, *474*, 64.
[15] W. Li, B. Chen, C. Meng, W. Fang, Y. Xiao, X. Li, Z. Hu, Y. Xu, L. Tong, H. Wang, W. Liu, J. Bao, Y. R. Shen, *Nano Lett.* **2014**, *14*, 955.
[16] C. T. Phare, Y.-H. Daniel Lee, J. Cardenas, M. Lipson, *Nature Photon.* **2015**, *9*, 511.
[17] Z. Shi, L. Gan, T.-H. Xiao, H.-L. Guo, Z.-Y. Li, *ACS Photon.* **2015**, *2*, 1513.
[18] Z. Sun, T. Hasan, F. Torrisi, D. Popa, G. Privitera, F. Wang, F. Bonaccorso, D. M. Basko, A. C. Ferrari, *ACS Nano* **2010**, *4*, 803.
[19] P. Avouris, *Nano Lett.* **2010**, *10*, 4285.
[20] T. Gu, N. Petrone, J. F. McMillan, A. v. d. Zande, M. Yu, G. Q. Lo, D. L. Kwong, J. Hone, C. W. Wong, *Nature Photon.* **2012**, *6*, 554.
[21] D. Popa, Z. Sun, F. Torrisi, T. Hasan, F. Wang, A. C. Ferrari, *Appl. Phys. Lett.* **2010**, *97*, 203106.
[22] X. Li, Y. Zhu, W. Cai, M. Borysiak, B. Han, D. Chen, R. D. Piner, L. Colombo, R. S. Ruoff, *Nano Lett.* **2009**, *9*, 4359.
[23] Q. Bao, K. P. Loh, *ACS Nano* **2012**, *6*, 3677.
[24] D. K. Armani, T. J. Kippenberg, S. M. Spillane, K. J. Vahala, *Nature* **2003**, *421*, 925.
[25] A. C. Ferrari, J. C. Meyer, V. Scardaci, C. Casiraghi, M. Lazzeri, F. Mauri, S. Piscanec, D. Jiang, K. S. Novoselov, S. Roth, A. K. Geim, *Phys. Rev. Lett.* **2006**, *97*, 187401.
[26] M. Cai, O. Painter, K. J. Vahala, *Phys. Rev. Lett.* **2000**, *85*, 74.
[27] H. Rokhsari, K. J. Vahala, *Phys. Rev. Lett.* **2004**, *92*, 253905.
[28] J. Yao, M. C. Wu, *Opt. Lett.* **2009**, *34*, 2557.

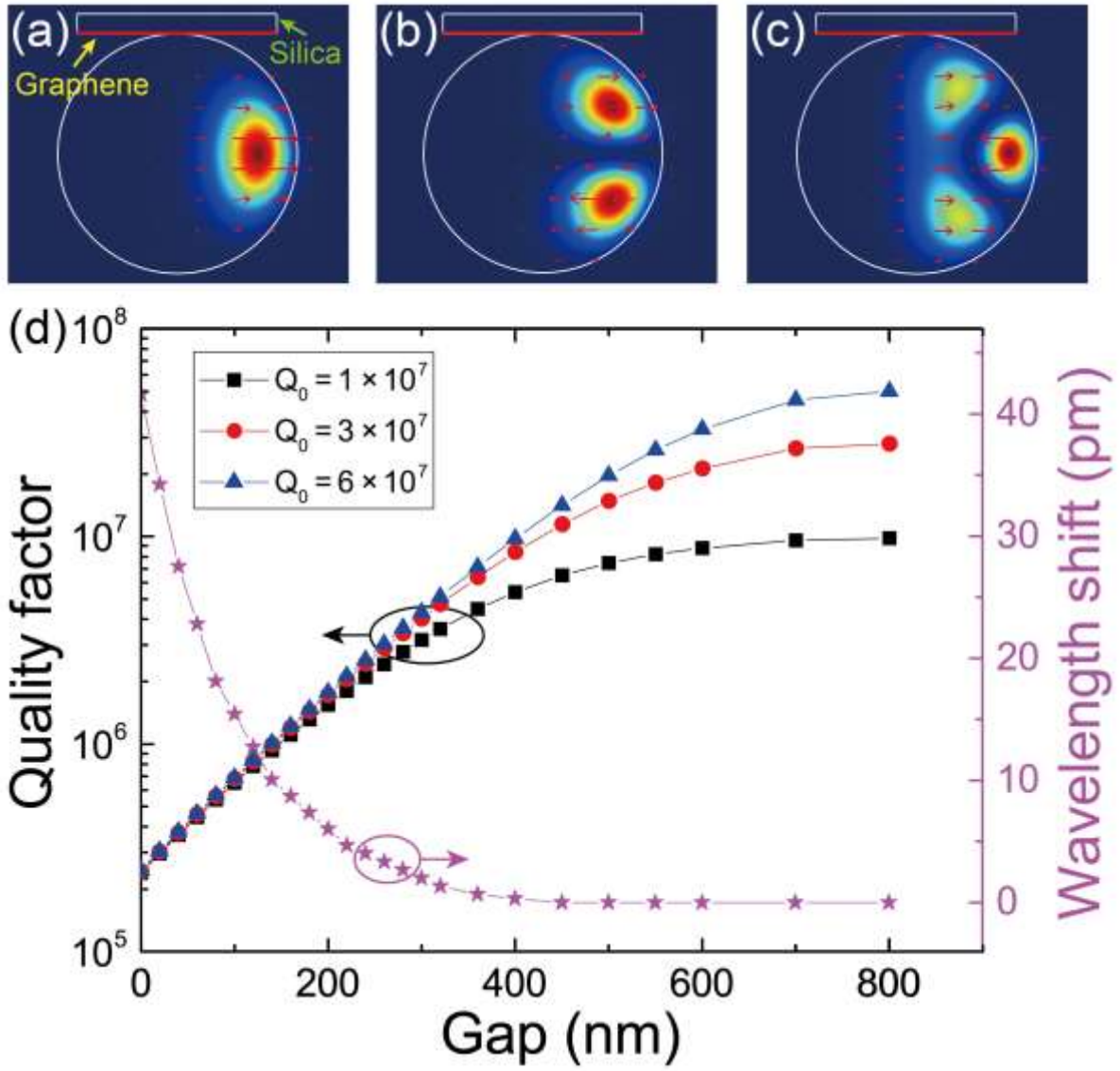

Figure 1. (a-c) Optical profiles of fundamental, second-order, and third-order TE modes of the fabricated microtoroid, respectively. (d) The simulated changes of the microcavity Q factor as well as the resonant wavelength shift as a function of the gap separation distance for the case of (1b). As one can see, when the gap vanishes, the ultimate Q eventually approaches the same value, approximately 2.3×10^5, for three different Q_0 (1×10^7, 3×10^7, and 6×10^7). The maximal shift is around 41 pm.

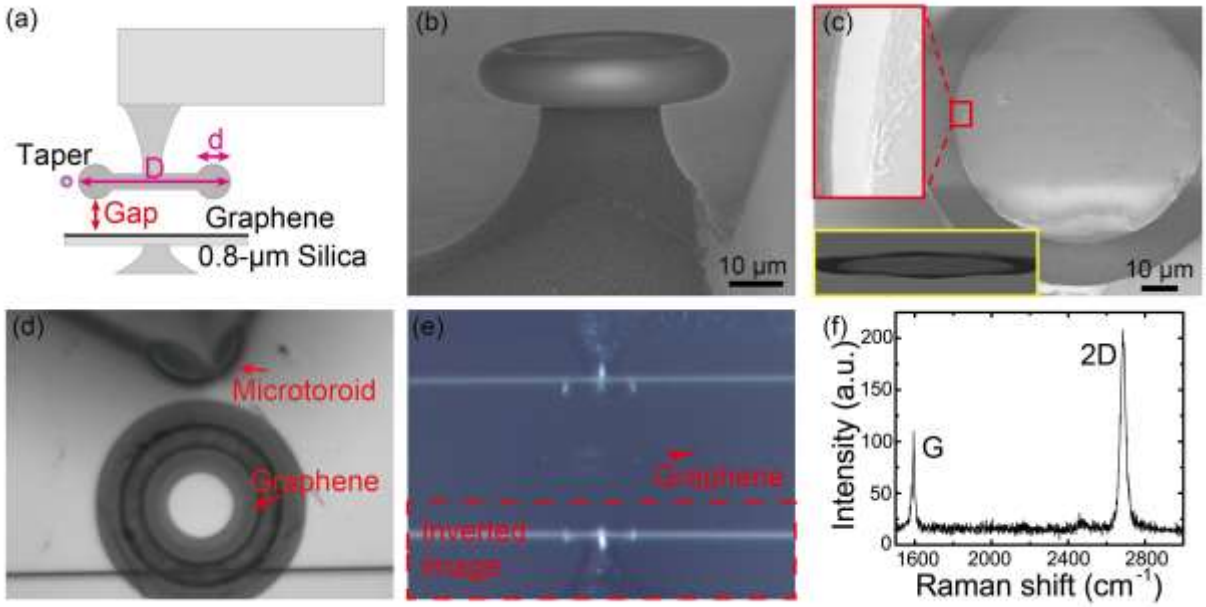

Figure 2. (a) Schematic of the experimental setup where the hybrid structure is composed of a microtoroid cavity and a graphene monolayer. The microtoroid was inverted for the convenience of observation and measurement. (b) The scanning electron micrograph of the microtoroid fabricated on the corner of a silicon wafer. (c) Top-view scanning electron micrograph of a specially designed microdisk coated with graphene monolayer. Insets: zoomed side-view and magnified images of the microdisk. (d-e) Top- and side-view optical microscope images of the hybrid structure, respectively. (f) Raman spectrum measured at the wavelength of 532 nm to verify that only one graphene monolayer is coated on the microdisk.

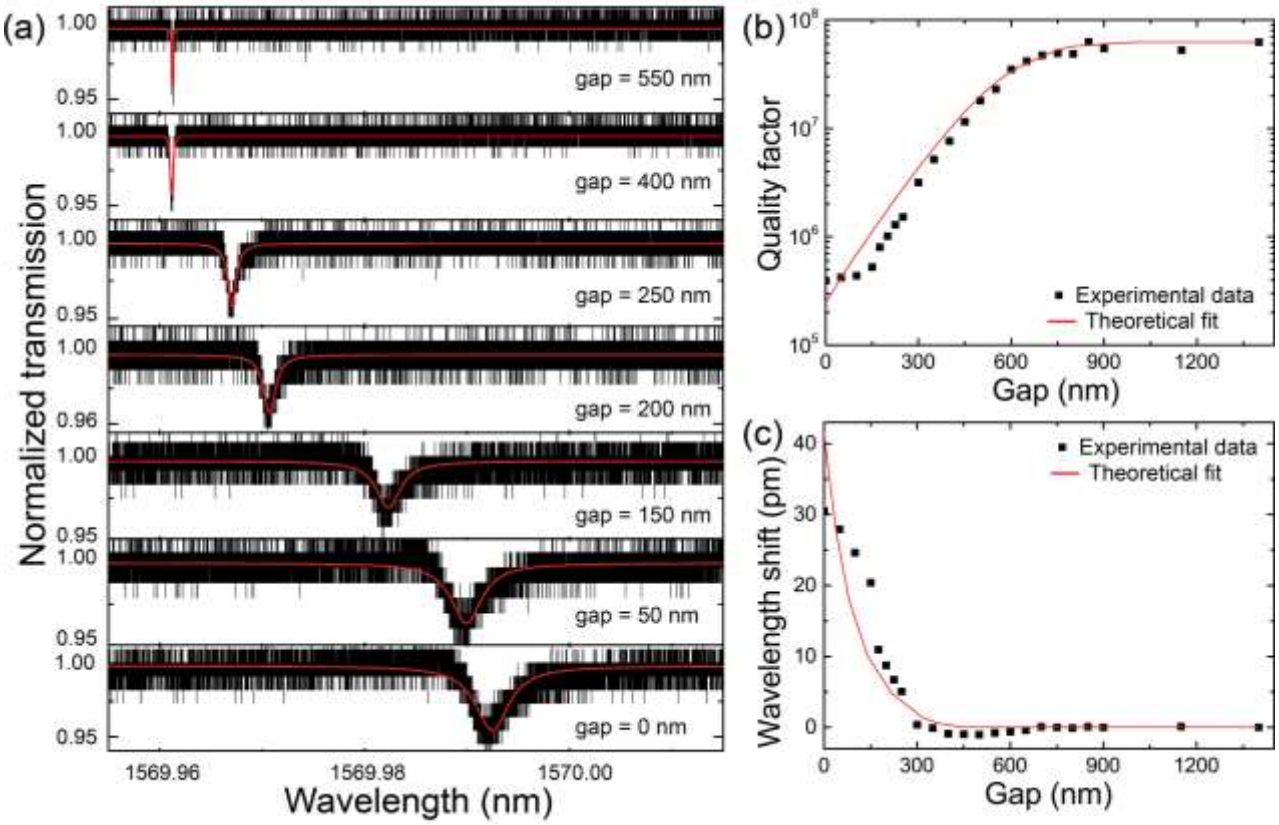

Figure 3. (a) Output transmission spectra as a function of the gap between graphene and microtoroid. (b-c) The extracted Q factor and the resonant wavelength shift of the microtoroid versus the gap. Red curves are the theoretical fits obtained from the finite-element simulation.

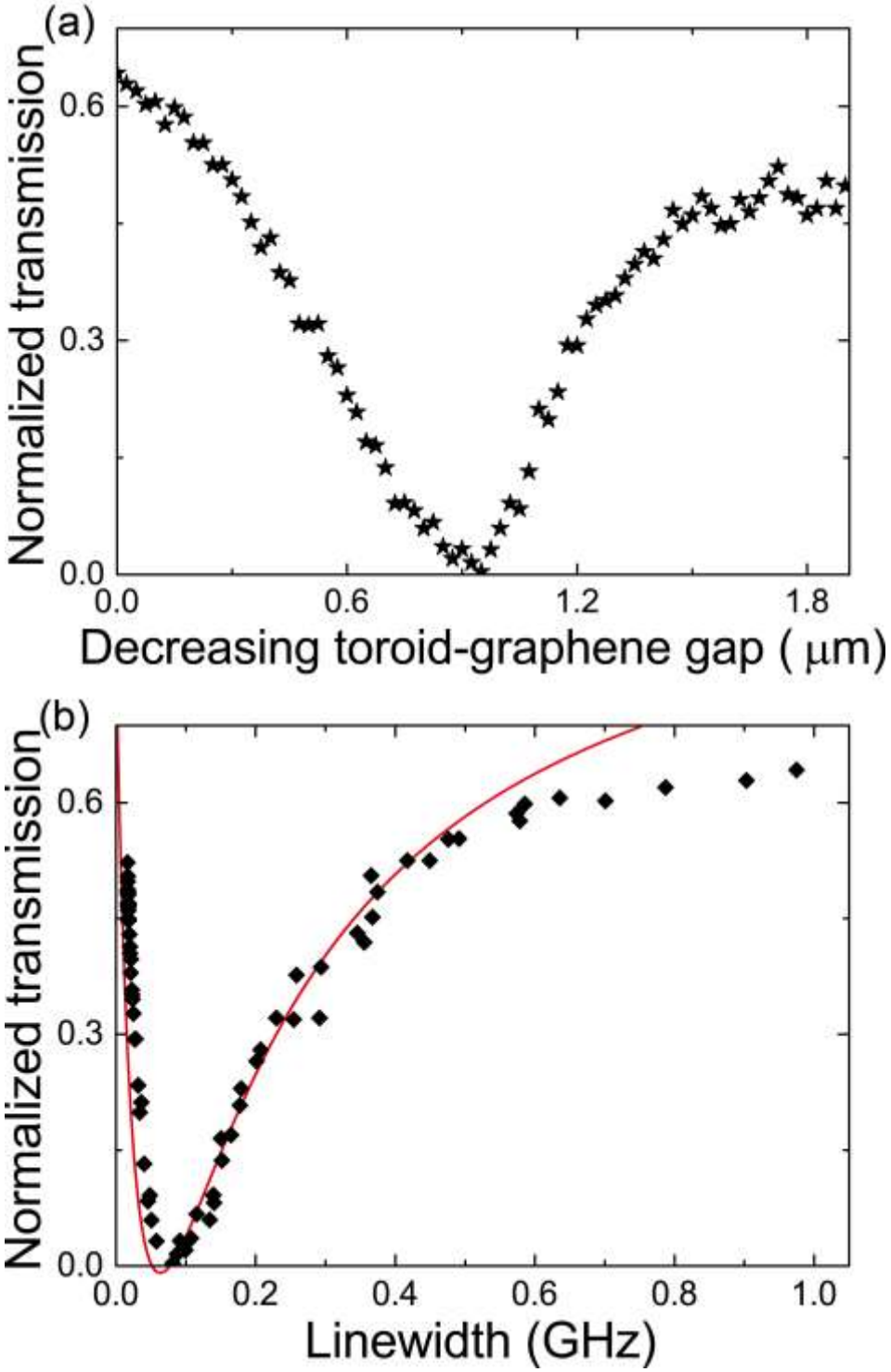

Figure 4. (a) Normalized transmission versus the gap between graphene and microcavity. The minimum transmission corresponds to the critical coupling point. (b) Normalized transmission versus the linewidth (FWHM) of the resonant mode. The red curve was calculated from the model given in Ref. [26].

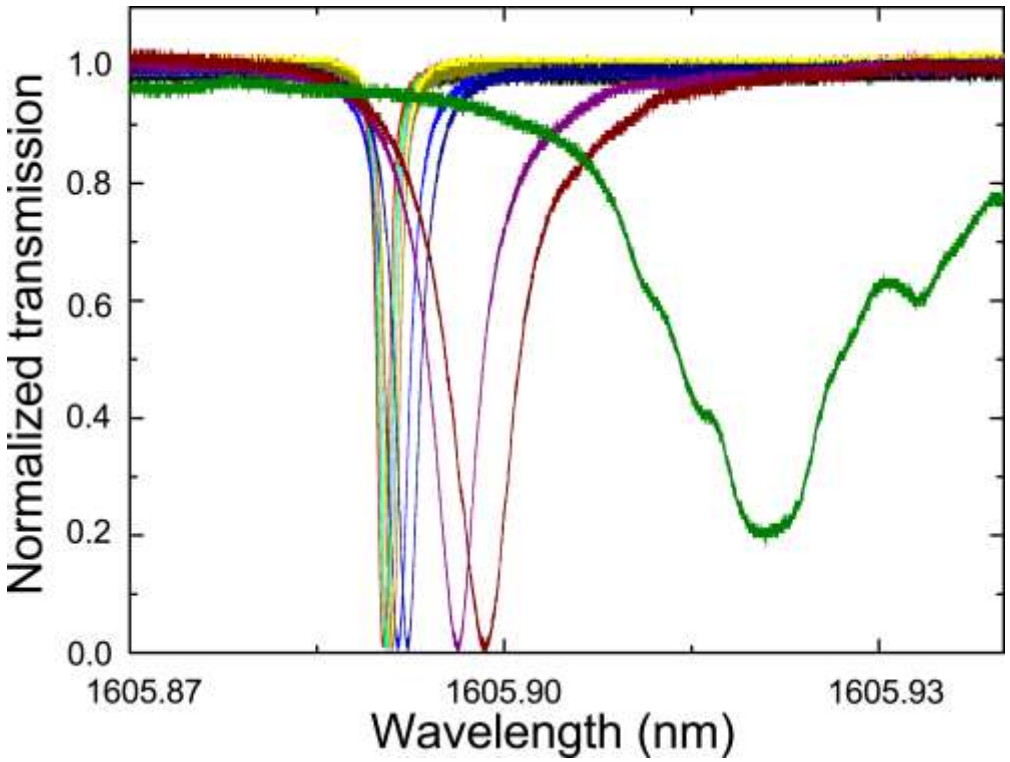

Figure 5. By tuning the gap, the large variations of the linewidth and resonant wavelength shift are used to realize a tunable optical filter with a tunable bandwidth in the range of 116.5 MHz ~ 2.2 GHz.

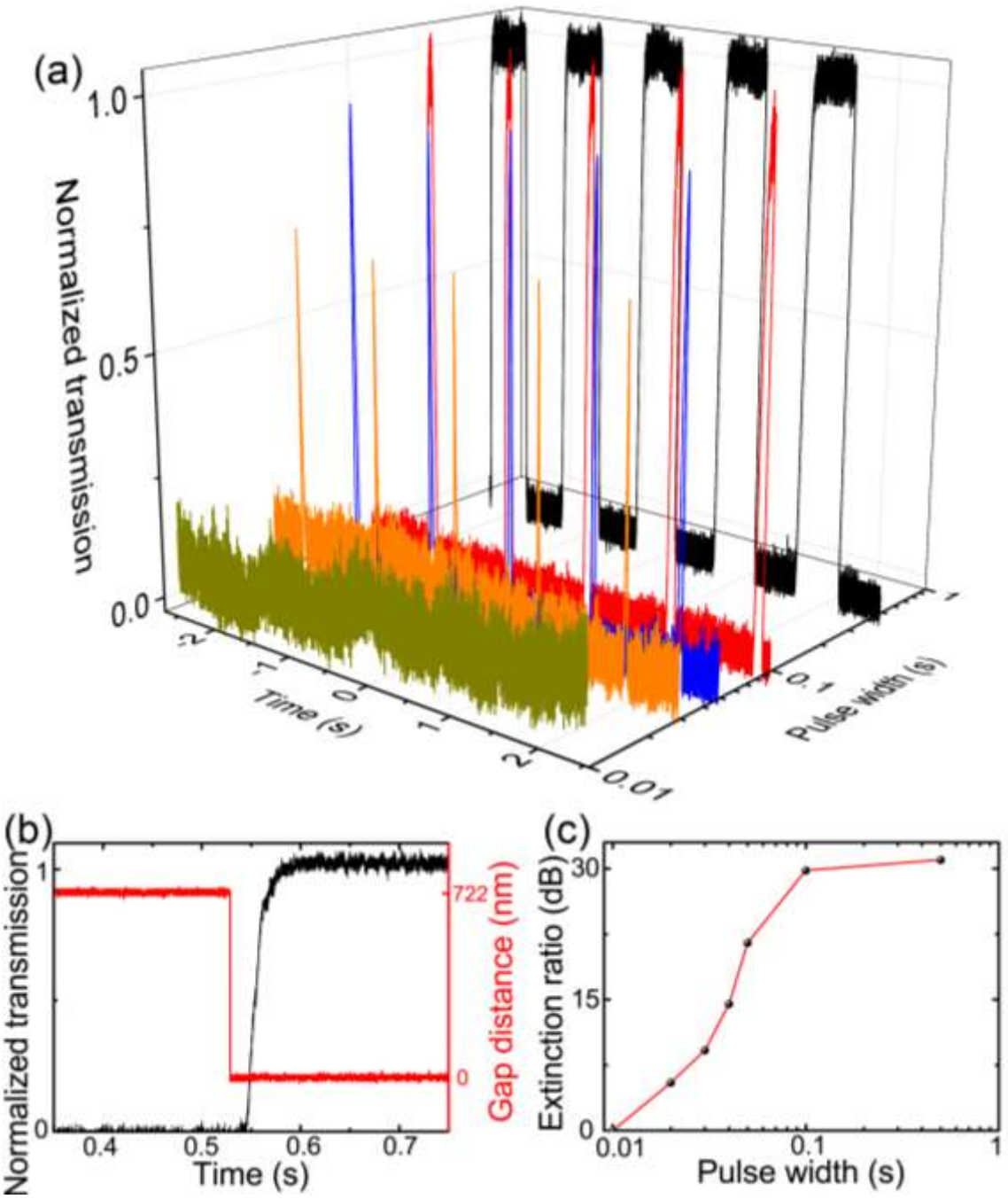

Figure 6. (a) Normalized transmission spectra of the demonstrated optical switch, where the peaks drop from maximum to almost 0 when the pulse width of the rectangular wave decreases from 0.5 s to 0.01 s. (b) Amplified transmission spectrum obtained for the 0.5-s pulse width of the rectangular wave. (c) The extinction-ratio change in (a) as a function of the pulse width, with the maximum of 31 dB.

The table of contents entry

This work presents a systematic study of controllable coupling between an ultra-high-Q microtoroid and a graphene monolayer. The microcavity Q can be dramatically changed by the efficient graphene absorption. The system is an excellent platform for realizing the tunable optical filter and optical switch with high extincation ratio. These results suggest our system a perfect scheme for realizing integrated opto-electronic devices including optical modulators.

Huibo Fan, Xun Zhang, Hao Li, Jinyi Zhao, Xiaoshun Jiang,* Yong Hu, Shiyue Hua, and Min Xiao

Controllable coupling between ultra-high-Q microtoroid and graphene for filtering and switching applications